Performance Study on Commercial Magnetic Sensors for Measuring Current of Unmanned Aerial Vehicles

Ke Zhu, Xuyang Liu, *Student Member, IEEE*, and Philip W. T. Pong, *Senior Member, IEEE*

***Abstract*— The industrial investment in unmanned aerial vehicles (UAVs) is soaring due to their multiple autonomous applications, such as aerial photography, rescue operations, surveillance, and scientific data collection. Current sensing is critical for determining battery capacity in charging and discharging process and alerting for system fault during the flight. Shunt resistors and Hall-effect sensors are traditionally used in UAVs. Recently, magnetoresistive (MR) sensors are gaining enormous attention from researchers. MR sensors tend to consume less power, and they are smaller in size than the Hall-effect sensors. In this paper, a number of off-the-shelf MR sensors were investigated to evaluate the possibility of applying them for UAVs. Another type of magnetic sensor (fluxgate) and shunt resistor was also studied and compared as a reference. The relative scoring method is adopted to evaluate the sensor performance under different metrics, and the results disclose that the MR sensors are highly suitable for current sensing of UAVs due to their higher accuracy, lower energy consumption, wider temperature endurance, smaller size, and less weight than other magnetic current sensors. They are also very competitive with traditional shunt resistors through the overall comparison. The remanence, thermal stability, and cross-field sensitivity of MR sensors are further discussed. This finding provides insight into the selection strategy of current sensors for UAVs and can enhance the industrial development of UAV potentially.**

***Index Terms*— Fluxgate sensor, Hall-effect sensor, magnetoresistive (MR) sensor, shunt resistor, unmanned aerial vehicles (UAVs).**

I. Introduction

THE global interest for unmanned aerial vehicles (UAVs) is growing rapidly (the UAV market is valued at U.S. $18.14 billion in 2017 and is projected to reach U.S. $52.30 billion by 2025 [2]) in both military and civilian operations. UAVs have found many applications, such as condition monitoring, geographical mapping, and performing certain dangerous tasks, wherein the sensor technologies are indispensable for achieving these functions [3]–[7]. These sensors include accelerometers, tilt sensors, engine intake flow sensors, magnetic sensors (electronic compasses), and current sensors [8]. Among these sensors, current sensors play an important role for a healthy operation of UAVs such as to prevent overcharging and safeguard against overcurrent [9], [10].

Four physical principles are typically applied for current sensors, namely Ohm's law (shunt resistors), Faraday's law of induction (search coils), Faraday effect (fiber-optic current sensors), and magnetic-field sensing (e.g., Hall-effect sensors). Since search coils only work with ac current and fiber-optic current sensors are bulky and expensive, they are not suitable for UAVs. Traditionally, shunt resistors [11], [12] and Hall-effect sensors [13]–[15] are commonly used in UAVs. However, they are not totally satisfactory in the application of UAVs. The shunt resistors dissipate the heat in the circuitry of UAVs [16], [17]. The Hall element is typically amplified with a conditioning circuit to improve its output, thereby increasing the size and weight of the Hall-effect sensor [18]. Thereby, it is worthwhile to seek a more suitable current sensor for UAVs.

Recently, magnetoresistive (MR) sensors are gaining enormous attention by researchers [19]. MR sensors tend to consume less power, and they are smaller in size than the Hall-effect sensors. In this paper, a number of off-the-shelf MR sensors were investigated to evaluate the possibility of applying them for UAVs. Another type of magnetic sensor (fluxgates) and shunt resistor was also studied and compared as a reference. Apart from measurement accuracy, the other parameters related to UAV performance, such as energy consumption, supply voltage, linear range, operating temperature, size and weight, cost of sensors, and measurement mode (invasive or noninvasive), are also discussed [20]. The rest of this paper is organized as follows. In Section II, several aspects of current sensors for UAVs are present. The sensors under study and their performance metrics are analyzed, respectively, with the relative scoring method in Section III. Section IV provides the overall comparison in different applications of UAVs for MR sensors, Hall-effect sensors, fluxgate, and shunt resistor and discusses the remanence, thermal stability, and cross-field sensitivity of MR sensors. The significance of this research is also disclosed. The final conclusion is drawn in Section V.

Manuscript received December 27, 2018; revised March 6, 2019; accepted March 27, 2019. Date of publication April 11, 2019; date of current version March 10, 2020. This work was supported in part by the Seed Funding Program for Basic Research, the Seed Funding Program for Applied Research, and the Small Project Funding Program from The University of Hong Kong, in part by the ITF Tier 3 Funding under Grant ITS/203/14, Grant ITS/104/13, and Grant ITS/214/14, in part by the RGC-GRF Grant under Grant HKU 17210014 and Grant HKU 17204617, and in part by the University Grants Committee of Hong Kong under Contract AoE/P-04/08. This paper was presented at the IEEE International Instrumentation and Measurement Technology Conference [1]. The Associate Editor coordinating the review process was Bruno Ando. *(Corresponding author: Philip W. T. Pong.)*

The authors are with the Department of Electrical and Electronic Engineering, The University of Hong Kong, Hong Kong (e-mail: zhuke@connect.hku.hk; liuxy@eee.hku.hk; ppong@eee.hku.hk).

Color versions of one or more of the figures in this article are available online at http://ieeexplore.ieee.org.

Digital Object Identifier 10.1109/TIM.2019.2910339

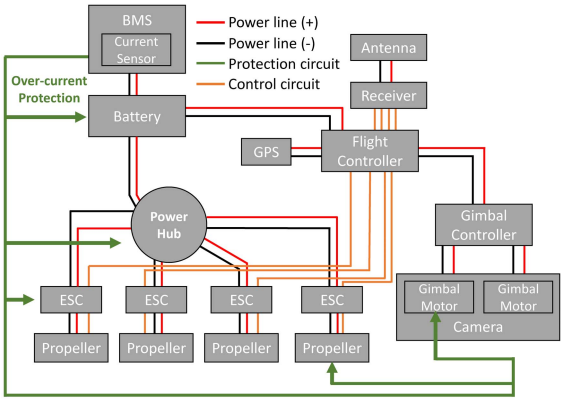

Fig. 1. Circuitry of a UAV, including the battery management system (BMS), current sensor, battery, power hub, electronic speed controller (ESC), propeller, and so on [3].

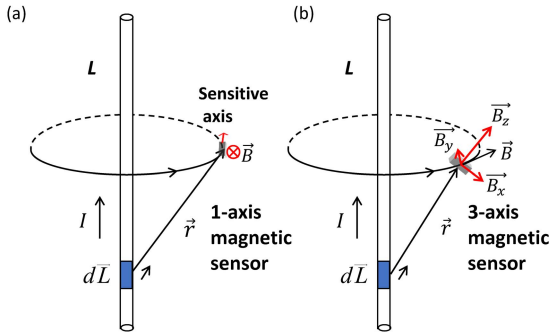

Fig. 2. Layout for the current-carrying conductor and a magnetic sensor. (a) Sensitive axis of a one-axis magnetic sensor must be tangential to the center axis of the current-carrying conductor. (b) Orientation of a three-axis magnetic sensor related to a current-carrying conductor can be arbitrary and flexible.

II. Performance Metrics

The UAVs undergo various power profiles in different parts of the UAV mission, such as takeoff, hovering, and landing. The accuracy of current sensing is critical, as they undertake the following tasks (see Fig. 1). First, with real-time current monitoring, the current sensors provide the volume of stored energy for the protection circuit to prevent overcharging during the charging process. The overcharging condition should be totally avoided because it can generate the heat and gases in batteries, resulting in the irreversible damage [21]. Second, the current sensors can measure the energy consumption of batteries for determining the remaining flight time [22]. In UAVs, the flight time is critically dependent on the battery life. A "dead stick" condition in which the battery becomes completely drained during flight can be disastrous [23]. Finally, the real-time current measured by current sensors can be used by the protection system to alert when there is a system fault [24]. As such, the accuracy of current sensing is an indispensable indicator for current-sensor performance.

Apart from the accuracy, there are other important performance metrics for current sensing. First, though typically only around 5% of total energy is spent on the sensing system of UAVs [25], every consumption counts considering by far, most commercial UAVs cannot fly continuously for more than half an hour without recharging. It is worthwhile to reduce the energy consumption of current sensing, which is also powered by the battery in order to sustain a longer flight time of UAVs. Second, the current flowing of UAVs can reach up to tens of amperes when they drive to the full throttles [9]. The current sensors should be capable of detecting large as well as small currents without any distortion, and therefore, a large linear range is preferred. Third, the current sensors can be exposed to harsh environments when the UAVs conduct tasks, such as firefighting and snowfield photographing. For example, the surface fire on the forest floor can reach up to 800 °C [26], and the air temperature in a snowing environment can be tens of degrees below zero [27]. Thus, the current sensors need to have a wide operating temperature range. Moreover, flight time is not solely dependent on battery capacity but also on the weight of a UAV [28]. A small and light current sensor can improve the compactness of UAVs, make the design of UAVs more flexible, and help enhancing the flying performance. Furthermore, commercial UAVs typically cost hundreds of USD [29]. Current sensors of lower costs can lead to a decrease in the overall cost of UAVs, which can make them more affordable for widespread utilization. Finally, the measurement mode (i.e., contact with the original circuit or not) of sensors is also discussed [16].

As such, the above-mentioned parameters, including accuracy, energy consumption, linear range, operation temperature, size, weight, cost, and measurement mode, are discussed for comparing the performance of current sensors.

III. Comparison Analysis

A. Sensors Under Study

The investigated off-the-shelf sensors included an anisotropic MR sensor (AMR), a tunneling magnetoresistance (TMR) sensor, a giant magnetoresistance (GMR) sensor, and open-loop Hall-effect sensors. Based on the Biot–Savart law, the sensitive axis of a one-axis MR sensor must be in the tangential direction in order to measure the magnetic field emanated from the current conductor, which is used to inversely work out the current in the conductor [see Fig. 2(a)]. However, a three-axis MR sensor does not have this restriction. The orientation of the three-axis MR sensor related to the conductor can be arbitrary since the magnitude of resultant magnetic fields ($\vec{B}$) can be calculated from the three mutually orthogonal sensing axes [($\vec{B}_x$, $\vec{B}_y$, and $\vec{B}_z$, see Fig. 2(b)]. This flexibility in orientation may be advantageous on the UAVs, which have limited space for hardware installation. As such, both commercial one- and three-axis MR sensors were tested. Another type of magnetic sensor (fluxgates) and shunt resistor was also studied as a comparison reference. Table I lists the specific magnetic sensors and shunt resistors that were studied in this paper.

B. Comparison Approach

The goal of this paper is to find the best current sensors for UAVs among several candidates by considering their performance metrics. Since the unit in each performance metric is different (e.g., volt for voltage, ampere for current, and so on),

TABLE I
LIST OF MAGNETIC SENSORS AND SHUNT RESISTOR FOR COMPARISON AS CURRENT SENSORS FOR UAVS

Sensor		Manufacturer	Remark	
AMR	HMC1051Z	HONEYWELL	1-axis	Thin film
	HMC1043L	HONEYWELL	3-axis	
TMR	TMR2301	Multi Dimension	3-axis	Spin valve
	TMR9002	Multi Dimension	1-axis	
GMR	AA002	NVE CORPORATION	1-axis	Multilayer
	GF708	SENSITEC	1-axis	Spin valve
Hall effect	CS-45AL	PANUCATT DEVICES	Open loop	
	ACS712	ALLEGRO	Open loop	
Fluxgate	FGM-3	SPEAKE & Co LIANFAPLEY	/	
Shunt resistor	CRS1050	ARCOL	/	

and the scale of each performance metric can be very various (e.g., the power consumption can only be several joules but price of sensors can be hundreds), it is not appropriate to simply sum up the value of each performance metric for comparison. The relative scoring algorithm [30] was adopted for comparing the performance of these current sensors. This method is suitable for a ranked list, which requires scoring multiple metrics for each player on the list, making it possible to consolidate scores from multiple metrics into a single score. The method is mathematically expressed as [30]

$$k(i) = 100 - \left[\frac{|x_i - Y|}{\sum_{i=1}^{N} x_i} \times 100 \right] \tag{1}$$

where $k(i)$ is the score of the evaluated item, N is the number of players, x_i is the value of the ith object, and Y represents the best value. This method converts the raw values of each parameter into a number between 0 and 100 while retaining the ranking order of the raw values. Also, this metric indicates how far ($|x_i - Y|$) the object value is from the best value. After obtaining the relative score of each metric, the final composite score can be summed up from these relative scores based on different weights under different demands of users. The overall performance of these current sensors for the UAVs can then be compared and analyzed.

C. Scoring

1) Accuracy: The accuracy is evaluated by the discrepancy between the consumed energy of the UAV measured by the sensor and the reference measured by an ammeter (Model 2000, Keithley). The battery voltage was measured by a multimeter (Model 34401, Hewlett Packard). The smaller the relative error, the better the sensing accuracy. The relative error of the consumed energy (ε) in this paper was measured experimentally over an operation time of the UAV, and it is defined as

$$\begin{aligned} \varepsilon &= \frac{|E_1 - E_2|}{E_2} \times 100\% \\ &= \frac{\left|\sum I_1^2(t_i)R - \sum I_2^2(t_i)R\right|}{\sum I_2^2(t_i)R} \times 100\% \\ &= \frac{\left|\sum I_1^2(t_i) - \sum I_2^2(t_i)\right|}{\sum I_2^2(t_i)} \times 100\% \end{aligned} \tag{2}$$

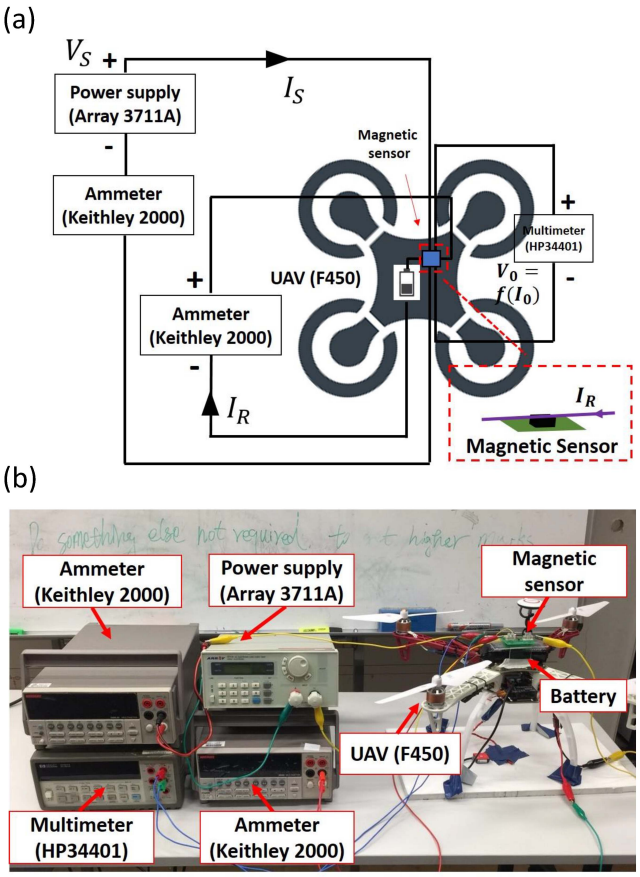

Fig. 3. Experimental setup to study the accuracy of magnetic sensors. (a) Electric circuit measuring UAV current (I_R), the output voltage (V_0) of the magnetic sensor, and working current (I_s) under typical supply voltage (V_s) of the magnetic sensor. (b) Hardware for measuring the accuracy of magnetic sensors.

where E_1 is the energy consumption based on sensor measurement, E_2 is the reference energy consumption, R is the equivalent resistance of UAVs, $I_1(t_i)$ is the current measured by the current sensor at a time point (t_i), and $I_2(t_i)$ is the reference current at the same point.

The circuit for measuring the relative error of current sensors is shown in Fig. 3, where a magnetic sensor is taken as an example. The sensor was placed in the proximity of the conductor carrying the current of the UAV [see Fig. 3(a)]. The battery current of UAV measured by the ammeter (Model 2000, Keithley) was taken as reference current (I_R). The sensor output (V_0) was measured by a multimeter (Model 34401, Hewlett Packard) to determine the sensing current of the sensor (I_0). During the measurement, the sensor was operating under their typical supply voltages (V_S) as specified on the datasheet. The hardware of the platform can be found in Fig. 3(b). The details of the tested UAV and the battery (see Fig. 4) are introduced as follows.

1) *UAV:* The tested UAV is a quadcopter (F450) from DJI company [31] [see Fig. 4(a)]. This model is widely used for aerial filming and photographing. It is equipped with a NAZA GPS System and controlled by RadioLink 2.4-GHz AT9 Radio System to adjust the throttle.
2) *Battery:* The lithium polymer battery [see Fig. 4(b)] was used in the UAV. Three cell batteries were bundled in

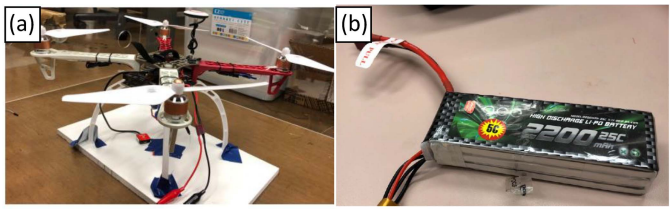

Fig. 4. UAV under test. (a) Quadcopter. (b) Lithium polymer battery (2200 mAh) to operate the UAV.

parallel to provide a rate voltage of 11.1 V. The total capacity was 2200 mAh, which was adequate for about 20-min operation of the UAV.

The UAV was operated for an acceleration duration of climbing up (the throttle was set from 0% to 40%) and also a deceleration duration of descending (the throttle was set inversely from 40% to 0%) [32]. The currents measured by the ammeter under these different throttles are plotted in Fig. 5(a). It can be seen that the current varied under different throttles, and it became larger under a larger throttle. The current measurement by using the magnetic sensor (GF708) as an example is plotted in Fig. 5(b), in which the current measurement by the sensor is similar to the measurement result by the ammeter. The real-time errors between them can be found in Fig. 5(c). The errors for AMR (HMC1043L) and shunt resistor (CRS1050) are also shown in Fig. 5(d) and (e), respectively. The error of the UAV energy consumption measured by the GF708 as defined by (2) was calculated as 0.684%. All the current sensors were tested under the same measurement, and the results for the error of consumed energy are displayed in Fig. 5(f). The results show that the sensing performance of sensors varies from one to another. However, the MR sensors tend to have less error of consumed energy than the Hall-effect sensors and the fluxgate sensor in general.

The rankings and relative scores of the tested sensors are calculated in Table II. It shows that the error of the UAV energy consumption for the MR sensors are generally smaller than the Hall-effect sensors (an average score of MR sensors is 96.57, while 89.92 for Hall-effect sensors). This can be attributed to the fact that the MR sensors have a higher sensing resolution than the Hall-effect sensors (e.g., the equivalent current for the 120-μgauss resolution of HMC1051Z is 0.06 mA at 5-mm sensing distance and hundreds of mA for ACS712 [33]). The error of the shunt resistor is the smallest (the score is 100), and this proves its advantage as a traditional current sensor. The fluxgate sensor performs the worst (the score is 55.86) because its sensing range (0–2 A) is typically limited [34] and it was not sufficient for this experiment (0–5.5 A), which increased the sensing error.

2) Energy Consumption: The sensor energy consumption describes the energy consumed by the sensor during the current measurement of the UAV. It is better to consume less energy since this energy is drawn from the battery of UAVs. The reasons why using the "energy consumption" of a sensor rather than its power in the comparison metric is that the operating powers of some sensors are not constant. For example, the power of shunt resistor changes with the current flowing through the conductor ($P = I^2R$, where I is the flowing current of the shunt resistor, R is its resistance, and P is its operating power). For the MR sensors, their resistances vary with the magnetic field emanated from the sensing current, and thus, their operating powers also change with the sensing current ($P = U^2/R$, where U is the supply voltage of the MR sensor, R is its resistance, and P is its operating power). The energy consumption is measured over the 14-min flying time in an experiment [see Fig. 5(a)]. The sensor energy consumption was calculated by the integration of supply voltage (V_s) and working current (I_s) over time. The power and energy consumption of the magnetic sensor (GF708) is plotted in Fig. 6(a) as an example. The energy consumption of all the sensors can be found in Fig. 6(b).

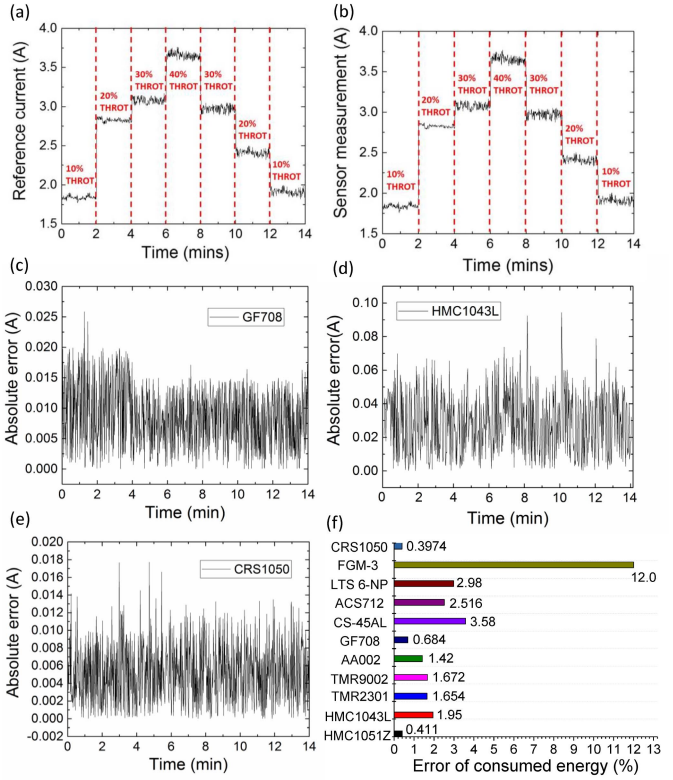

Fig. 5. Error of UAV energy consumption measured by current sensors under the flight of UAV with varied throttle settings. (a) Current measured by the ammeter (Model 2000, Keithley) during a flying mode of UAV (the throttle level was set as 10%, 20%, 30%, and 40% of the UAV). (b) Current measurement by GF708. (c) Current errors between the sensor measurement (GF708) and the reference value. (d) Current errors between the sensor measurement (HMC1043L) and the reference value. (e) Current errors between the sensor measurement (CRS1050) and the reference value. (f) Error of UAV energy consumption measured by current sensors.

TABLE II
ERRORS, RANKINGS, AND RELATIVE SCORES OF CURRENT SENSORS

Sensor		Error (%)	Ranking	Relative Score	
AMR	HMC1051Z	0.41	2	99.95	96.57 (avg.)
	HMC1043L	1.95	7	94.09	
TMR	TMR2301	1.65	5	95.22	
	TMR9002	1.67	6	95.15	
GMR	AA002	1.42	4	96.11	
	GF708	0.68	3	98.91	
Hall effect	CS-45AL	3.58	9	87.89	89.92 (avg.)
	ACS712	2.51	8	91.94	
Fluxgate	FGM-3	12	10	55.86	
Shunt resistor	CRS1050	0.40	1	100	

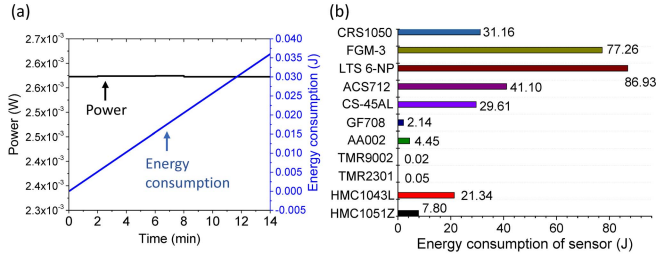

Fig. 6. Study of energy consumption for current sensors. (a) Power and energy consumption of GF708 during the operation of the UAV. (b) Energy consumption of current sensors under the test.

TABLE III
ENERGY CONSUMPTION, RANKING, AND RELATIVE SCORES OF CURRENT SENSORS

Sensor		Energy (J)	Ranking	Relative Score	
AMR	HMC1051Z	7.80	5	96.38	97.23 (avg.)
	HMC1043L	21.34	6	90.08	
TMR	TMR2301	0.05	2	99.99	
	TMR9002	0.02	1	100	
GMR	AA002	4.45	4	97.94	
	GF708	2.14	3	99.01	
Hall effect	CS-45AL	29.61	7	86.23	83.56 (avg.)
	ACS712	41.10	9	80.89	
Fluxgate	FGM-3	77.26	10	64.06	
Shunt resistor	CRS1050	31.16	8	85.51	

The Hall-effect sensor and the fluxgate sensor tend to cost more energy than the MR sensors.

The rankings and relative scores of sensors regarding the energy consumption are calculated in Table III. The MR sensors have a higher score on energy consumption (an average score of 97.23) than the Hall-effect sensors (an average score of 83.56). The MR sensors consumed less energy than the Hall-effect sensors because these commercial Hall-effect sensors are typically installed with some additional circuits (e.g., Hall current drive for ACS 712). The fluxgate sensor consumes a large amount of energy since an excitation coil is installed inside for generating the excitation fields [35]. The energy consumption of the shunt resistor depends on the currents flowing through it over time.

3) Linear Range: The linearity is the sensor's ability to respond linearly without hysteresis over its operating range. A high linearity is essential to provide an accurate measurement of the larger current. For the AMR, TMR, and GMR sensors, their linearity was calculated by the Biot–Savart law based on their saturation fields provided in the datasheet [36]–[41] and the distance between the current conductor and the sensor (5 mm in the experiment). For the commercial Hall-effect sensors, their linearity was provided in the datasheet. Regarding the fluxgate sensor (FGM-3), the linearity was determined experimentally at room temperature by wrapping the current conductor around its surface. The linearity of the shunt resistor (CRS1050) was attained based on its maximum power rating (7 W [42]) and resistance. The rankings and relative scores of sensors regarding the linear range in the room temperature are calculated in Table IV. The MR sensors and the shunt resistor obtained the highest score (i.e., 64.74 and 62.71, respectively) compared with the Hall-effect sensors (average score of 54.61) and the fluxgate sensor (the score of 51.59). The linearity of magnetic sensors depends

TABLE IV
LINEAR RANGE, RANKINGS, AND RELATIVE SCORES OF CURRENT SENSORS AT ROOM TEMPERATURE

Sensor		Maximum current (A)	Ranking	Relative Score	
AMR	HMC1051Z	**15**	7	54.12	64.74 (avg.)
	HMC1043L	**15**	7	54.12	
TMR	TMR2301	**250**	1	100	
	TMR9002	**20**	6	55.10	
GMR	AA002	**90**	2	68.77	
	GF708	**26.25**	4	56.32	
Hall effect	CS-45AL	**25**	5	56.08	54.61 (avg.)
	ACS712	**10**	8	53.15	
Fluxgate	FGM-3	**2**	9	51.59	
Shunt resistor	CRS1050	**59**	3	62.71	

TABLE V
TEMPERATURE RANGE, RANKING, AND RELATIVE SCORES OF MAGNETIC SENSORS

Sensor		Temperature range (°C)	Ranking	Relative Score	
AMR	HMC1051Z	**165**	3	96.03	96.14 (avg.)
	HMC1043L	**165**	3	96.03	
TMR	TMR2301	**165**	3	96.03	
	TMR9002	**165**	3	96.03	
GMR	AA002	**175**	2	96.69	
	GF708	**165**	3	96.03	
Hall effect	CS-45AL	**110**	5	92.38	92.88 (avg.)
	ACS712	**125**	4	93.38	
Fluxgate	FGM-3	**50**	6	88.41	
Shunt resistor	CRS1050	**225**	1	100	

TABLE VI
SIZE, WEIGHT, RANKING, AND RELATIVE SCORE OF CURRENT SENSORS

Sensor		Size (mm^3)	Ranking	Relative Score		Weight (g)	Ranking	Relative Score	
AMR	HMC1051Z	**92.16**	8	99.66	99.88 (avg.)	**0.160**	5	99.46	99.43 (avg.)
	HMC1043L	**10.50**	1	100		**0.026**	3	99.98	
TMR	TMR2301	**62.50**	6	99.79		**0.022**	2	99.99	
	TMR9002	**37.58**	4	99.89		**0.078**	4	99.78	
GMR	AA002	**30.48**	3	99.92		**0.694**	7	97.36	
	GF708	**11.70**	2	100		**0.021**	1	100	
Hall effect	CS-45AL	**13867.72**	10	43	71.42 (avg.)	**8.747**	9	65.80	81.04 (avg.)
	ACS712	**51.45**	5	99.89		**0.970**	8	96.28	
Fluxgate	FGM-3	**10067.82**	9	58.63		**14.590**	10	42.90	
Shunt resistor	CRS1050	**78.75**	7	99.72		**0.205**	6	99.28	

on their saturation fields, while the shunt resistor relies on its maximum rating power.

4) Operation Temperature: The rankings and relative scores of sensors regarding the operation temperature are calculated in Table V. The MR sensors (the average score is 96.14) outperform the Hall-effect sensors (the average score is 92.88). This is because the Hall-effect sensors exhibit considerable temperature drift [43]. The shunt resistor is much more stable (the score is 100.0), since its resistance is not easily affected by temperature, as it has a small temperature coefficient.

5) Size and Weight: A compact and light current sensor is beneficial for UAVs. The rankings and relative scores of sensors regarding the size and cost are calculated in Table VI. The MR sensors are more compact and lighter (the average score of 99.88 and 99.43 for size and weight, respectively) than the Hall-effect sensors (the average score of 71.42 and 81.04 for size and weight, respectively) and the fluxgate sensor (the score of 58.63 and 42.90 for size and weight, respectively). This is because the MR sensors do not need the external circuits, such as Hall-effect sensors (e.g., conditioning circuits) or the iron core of the flux gate sensor.

6) Cost: The whole cost of UAVs can be reduced if the current sensors cost less. The rankings and relative scores of sensors regarding the operation temperature are calculated

TABLE VII
COST, RANKINGS, AND RELATIVE SCORES OF CURRENT SENSORS

Sensor		Cost (USD)	Ranking	Relative Score	
AMR	HMC1051Z	33	6	90.96	81.00 (avg.)
	HMC1043L	49	8	85.72	
TMR	TMR2301	59	9	82.80	
	TMR9002	114	10	33.24	
GMR	AA002	8	3	97.67	
	GF708	15	4	95.63	
Hall effect	CS-45AL	17	5	95.04	96.94 (avg.)
	ACS712	4	2	98.83	
Fluxgate	FGM-3	42	7	88.34	
Shunt resistor	CRS1050	2	1	100	

in Table VII. The MR sensors are a bit more expensive (an average score of 81.00) than the Hall-effect sensor (an average score of 96.94). This is because tens of millions of Hall-effect devices are made each year for a high volume of application, making the price of Hall-effect sensors cheaper because of an economy of scale [44]. The shunt resistor is the cheapest (the score is 100.0) since it is just a simple resistor and the technology is very mature.

7) Measurement Mode: In contrast to the shunt resistors, the magnetic sensors measure the current without making physical contact with the original circuit. This noncontact feature is very beneficial when an external instrument is necessary to be connected for current measurement. However, the invasiveness of shunt resistors may not be a dominant disadvantage over magnetic sensors if the shunt resistors are already planned and integrated into the UAVs during the design stage. The measurement mode is thus not further taken into consideration in the overall comparison metrics.

IV. OVERALL COMPARISON AND DISCUSSION

A. Overall Comparison

Now, each relative score of comparative metrics for the MR sensors, Hall-effect sensors, a fluxgate sensor, and a shunt resistor is depicted by the radar graph approach [45] (see Fig. 7). This visualized graph can describe the strengths and weakness of sensors on each performance metric clearly. By comparing Fig. 7, we can obtain that the MR sensors outperform the Hall-effect sensors in many respects. This is mainly attributed to the thin-film material and the structure of MR sensors [46]. The Hall-effect sensors are typically made of silicon, while the MR sensors are of permalloy thin films [47]. Though they both respond to time-variant fields, MR sensors are roughly 100 times more sensitive than the Hall-effect sensors [47]. The power consumption of MR sensors is smaller than the Hall-effect sensors since MR thin films and structure can be fabricated with high resistance [46]. Both the Hall-effect and MR sensors are readily available in the market; however, MR sensors offer unique advantages, including smaller package size, lower power consumption, better thermal stability, and better resolution from Fig. 7 over the Hall-effect sensors for the battery-powered systems [48]. The MR sensors are envisioned to be the new solutions for future advanced sensing applications where advanced precision, lower power consumption, and tiny package size are required. The continuous technological advancement of MR sensors will result in the cost drop, and MR sensors may

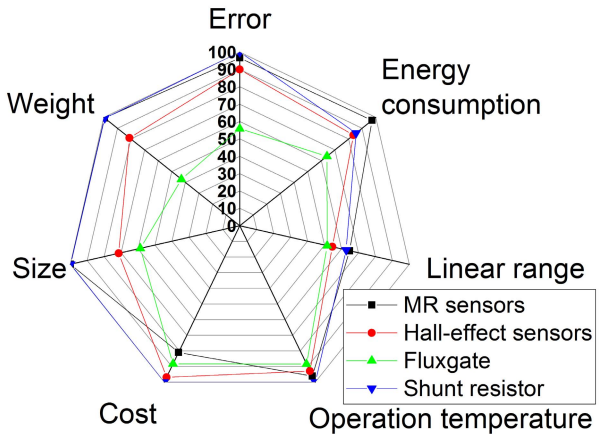

Fig. 7. Comparison of MR sensors, Hall-effect sensors, fluxgate, and shunt resistor by a radar graph.

invade the market share of Hall-effect sensors in the current sensor market.

It is worth mentioning that the overall score for the sake of selecting the best current sensor of UAVs depends on the specific demands of users. This can be calculated from summing up the relative score in each comparison metric based on the different weights, namely

$$\text{Score} = \sum_{i=1}^{N} w_i T_i \tag{3}$$

where w_i is the corresponding weight and T_i is the related score in the comparison metric. Two demonstrations are given for the cheap-mass-market and military-mission UAVs, respectively. The weights in comparison metrics are classified as "very important ($w_i = 7$)," "important ($w_i = 5$)," and "not so important ($w_i = 3$)." Regarding the cheap-mass-market UAVs, the buyers are amateurs who mainly concern about the cost, size, and weight ($w_i = 7$). They do not need their UAVs to carry out harsh tasks, and thus, they care less on operation temperature ($w_i = 3$). However, the error and energy consumption and UAVs are critical to military missions ($w_i = 7$). These users can afford the cost, size, and weight of UAVs ($w_i = 3$). Since the UAVs may carry out harsh tasks, a wide operation temperature is also important ($w_i = 5$). As the sensors can be linearized easily with microcontrollers (e.g., single linear approximation method or piecewise linear approximation method [49]), a lower weight is assigned to the linearization criteria ($w_i = 3$). The total scores of each sensor are summed up in Tables VIII and IX. The results depict that the traditional shunt resistors still perform the best among all sensors (i.e., 3508.68 and 2883.7 in cheap-mass-market and military-mission UAVs, respectively). However, the MR sensors are very competitive and achieving scores very close to those of shunt resistors (i.e., 3413.81 and 2872.45 in cheap-mass-market and military-mission UAVs, respectively). With more investment on MR sensors in the future, the cost of MR sensor will continue to decrease as the sales volume increases [44]. This will make the MR sensors as affordable as the shunt resistor. Therefore, it is believed that the MR sensors are highly deployable for the UAV applications and products in the future.

TABLE VIII
TOTAL SCORE FOR CHEAP-MASS-MARKET UAVS UNDER DIFFERENT WEIGHTS

Sensor	Error (5)		Energy consumption (5)		Linear range (3)		Operation temperature (3)		Cost (7)		Size (7)		Weight (7)		Total
	Score	Sub-total	Score	Sub-total	Score	Sub-total	Score	Sub-total	Score	Sub-total	Score	Sub-total	Score	Sub-total	
MR	96.57	482.85	97.23	486.15	64.74	194.22	96.14	288.42	81	567	99.88	699.16	99.43	696.01	3413.81
Hall-effect sensor	89.92	449.6	83.56	417.8	54.61	163.83	92.88	278.64	96.94	678.58	71.42	499.94	81.04	567.28	3055.67
Fluxgate	55.86	55.86	64.06	320.3	51.59	154.77	88.41	265.23	88.34	618.38	58.63	410.41	42.9	300.3	2125.25
Shunt resistor	100	500	85.51	427.55	62.71	188.13	100	300	100	700	99.72	698.04	99.28	694.96	3508.68

TABLE IX
TOTAL SCORE FOR MILITARY-MISSION UAVS UNDER DIFFERENT WEIGHTS

Sensor	Error (7)		Energy consumption (5)		Linear range (3)		Operation temperature (5)		Cost (3)		Size (3)		Weight (3)		Sum
	Score	Total	Score	Total	Score	Total	Score	Total	Score	Total	Score	Total	Score	Total	
MR	96.57	675.99	97.23	680.61	64.74	194.22	96.14	480.7	81	243	99.88	299.64	99.43	298.29	2872.45
Hall-effect sensor	89.92	629.44	83.56	584.92	54.61	163.83	92.88	464.4	96.94	290.82	71.42	214.26	81.04	243.12	2590.79
Fluxgate	55.86	391.02	64.06	448.42	51.59	154.77	88.41	442.05	88.34	265.02	58.63	175.89	42.9	128.7	2005.87
Shunt resistor	100	700	85.51	598.57	62.71	188.13	100	500	100	300	99.72	299.16	99.28	297.84	2883.7

B. Other Issues

Though the overall performance of MR sensors excels the Hall-effect sensor in the previous analysis of Section IV-A, some issues (i.e., remanence, cross-field sensitivity, and thermal stability of offset) still need to be addressed for MR sensors since they contain magnetic materials in contrast to the traditional shunt-resistor current sensor. The analysis with the experimental results of these aspects is explained as follows.

1) *Remanence:* The resistance of an MR sensor varies with the external magnetic field. If the external magnetic field is within the operational field range, the magnetization of the MR sensor will return to its original orientation after the field is removed. However, if the external magnetic field is beyond the operational field range, the remanence is left behind and the magnetization of the MR sensor does not return to its original orientation. The remanences of AMR, TMR, and GMR sensors (the output of Hall effect is proportional to the magnetic flux density present, and thus, Hall sensors do not exhibit remanence [50]) were studied by the experimental setup in Fig. 8(a). A sweeping magnetic field was generated by a Helmholtz coil. The measurement results can be found in Table X and Fig. 8. The remanences are 0.15 mV/V across ±0.6-mT sweep for AMR HMC1051Z, 22.83 mV/V across ±0.9-mT sweep for TMR TMR9002, 1.8 mV/V across ±1.5-mT sweep for GMR GF708, and 0.45 mV/V across ±3.0-mT sweep for GMR AA002. These remanences can affect the measurement accuracy of the sensors. To solve this problem, a strong restoring magnetic field can be applied momentarily to restore the sensor magnetization by using an on-chip current strap for remagnetization or flipping in sensor [51]. These set/reset pulse circuits can be integrated into the UAVs.
2) *Thermal Stability:* The temperature of a sensor indicates the percentage possible error in the measurement per unit (°C). As such, it is a critical factor in ensuring measurement accuracy, particularly in industrial applications where large temperature variations can occur. The thermal stability coefficient (TC) is calculated as [43]

$$TC = \frac{|V_{T1} - V_{T2}|}{|T_1 - T_2| \times V_{T1}} \times 100\ (\%/^{\circ}\mathrm{C}) \tag{4}$$

where V_{T1} is the output of the sensor at temperature T_1 and V_{T2} is the output of the sensor at temperature T_2. The thermal stability coefficients of AMR, TMR, GMR, and Hall-effect sensors were tested ($T_1 = 25$ °C and $T_2 = 120$ °C) and shown in Table X and Fig. 8. The thermal stability coefficients were 0.424%/°C for AMR HMC1051Z, 0.0908%/°C for TMR9002, 0.255%/°C for GMR GF708, 0.285%/°C for GMR AA002, and 0.009%/°C for Hall-effect sensor ACS712. The TMR sensor made of magnetic tunnel junction element exhibited better thermal stability than AMR and GMR sensors [52], [53]. The thermal stability coefficients of the Hall-effect sensor were the smallest because it was made of semiconductor materials (e.g., InAs). MR sensors still need to catch up with the Hall-effect sensor in this aspect; however, it is worth mentioning that great research efforts have been made in the last decades to enhance the robustness of MR sensors to over 200 °C (e.g., GMR sensors made of spin-valve systems comprising IrMn, PtMn, or NiMn with high blocking temperature [54]).
3) *Cross-Field Sensitivity:* MR sensors exhibit some form of cross-field response because they rely on the magnetostatic response of a free layer, and it can be influenced by the field in all directions [55], [56]. The cross-field responses of AMR, TMR, and GMR sensors were tested by the experimental setup (the sensor sensitive axis was in the x-axis) in Fig. 8(a). The results in Table X show that the sensitivity ratio of the cross field (y- and z-axes) to the sensitive field (x-axis) ranged from 2% to 7% for the MR sensors. In the real application of UAVs, this problem can be minimized by shielding in one

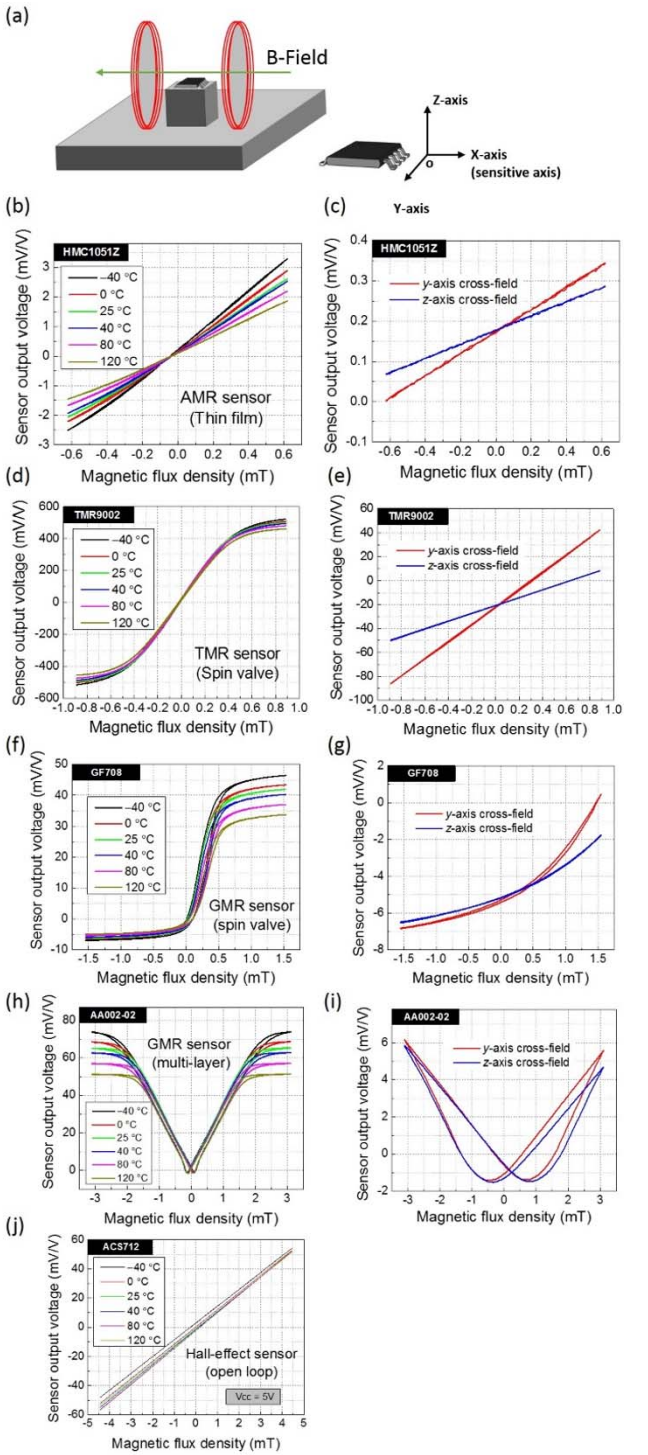

Fig. 8. Remanence, thermal stability, and cross-field sensitivity test of MR and Hall-effect sensors. (a) Experimental setup: the sensor was applied with an external magnetic field generated by a Helmholtz coil. (b) Remanence and thermal stability test for HMC1051Z. (c) Cross-field sensitivity test for HMC1051Z. (d) Remanence and thermal stability test for TMR9002. (e) Cross-field sensitivity test for TMR9002. (f) Remanence and thermal stability test for GF708. (g) Cross-field sensitivity test for GF708. (h) Remanence and thermal stability test for AA002. (i) Cross-field sensitivity test for AA002. (j) Thermal stability test for ACS712.

orientation and amplifying in the other by incorporating the magnetic flux concentrators (MFCs) [56], [57].

TABLE X

REMANENCE, THERMAL STABILITY, AND CROSS-FIELD SENSITIVITY STUDY OF AMR, TMR, GMR, AND HALL-EFFECT SENSORS

Sensor	Remanence (mV/V ,T= 25°C)	Thermal coefficient (%/°C)	Sensitivity (mV/V/mT)				
			X-axis	Y-axis	Y/X (%)	Z-axis	Z/X (%)
AMR (HMC1051Z, thin film)	0.15 (±0.6 mT)	0.424	3.85 (0 - 0.6 mT)	0.27	7%	0.18	5%
TMR (TMR9002, spin valve)	22.83 (±0.9 mT)	0.0908	1000.00 (0 - 0.4 mT)	72.36	7%	32.70	3%
GMR (GF708, spin valve)	1.8 (±1.5 mT)	0.255	80.00 (0 - 0.25 mT)	1.60	2%	1.60	2%
GMR (AA002, multi-layer)	0.45 (±3.0 mT)	0.285	33.00 (0 - 1.0 mT)	2.00	6%	1.75	5%
Hall-effect (ACS712, Open-loop)	/	0.009	11.49 (0 - 4.0 mT)	/	/	/	/

C. Significance to the UAV Industry

The signification of this paper can be summarized as follows. First, the current sensing of UAVs has been dominated by the shunt resistors [58] and the Hall-effect sensors [59]. Now, this paper has disclosed the possibility that they can be replaced by the MR sensors with better performance. The performance of commercial current sensors (including MR, Hall-effect sensors, fluxgate, and shunt resistor) in various aspects (error, energy consumption, linear range, operation temperature, cost, size, weight, and measurement mode) has been compared and analyzed. In this paper, the values of each sensor in comparison metric were attained from the literature and experiments and then evaluated by the modified relative scoring method. The results show that the MR sensors outperform the shunt resistors, Hall-effect sensors, and fluxgates in current sensing for UAV application in both cheap-mass-market and military-mission UAVs. Second, critical issues of magnetic sensors (i.e., remanence, thermal stability, and cross-field sensitivity) for applying MR sensors in current sensing for UAVs have been addressed. Most previous works reported the sensing performance of MR sensors in normal status (i.e., room temperature and unsaturated condition) [19], [55], [60]. However, the UAVs may be exposed to harsh conditions, such as a high-temperature working condition or environment with excessive and complicated background magnetic fields. As such, the performance of remanence, thermal stability, and cross-field sensitivity of these commercial magnetic sensors were studied and compared. Discussions on how to eliminate these problems (e.g., the set/reset pulse circuits for remagnetization to remove the remanence) are also provided. This paper addresses the practical challenges of utilizing MR sensors in current sensing for UAVs.

Traditionally, MR sensors have been mainly used as the electronic compass, altitude reference in UAVs (see Fig. 9). This paper has extended the application regime of MR sensors to current sensing in UAVs. As a new sensing technology, the MR sensors were discovered just several decades ago (i.e., TMR discovered in 1975 [61] and GMR discovered in 1988 [62]). They become available in a

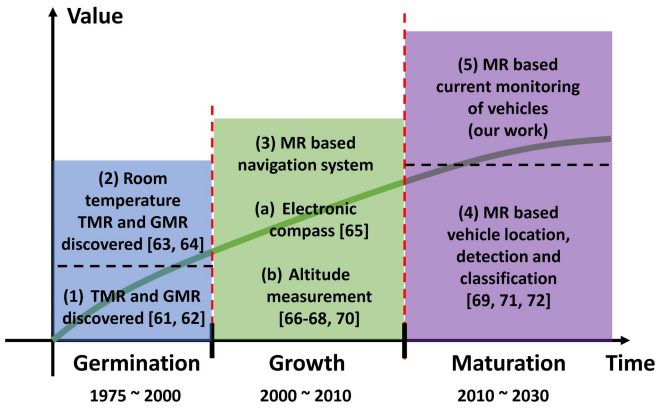

Fig. 9. Development of MR sensors in the application of UAVs over different time scales (germination, growth, and maturation).

series of applications after the room-temperature MR sensors are observed (i.e., the room-temperature GMR observed in 1991 [63] and TMR in 1995 [64]). Afterward, the MR sensors demonstrated their abilities as a basic electronic compass and altitude measurement between 2000 and 2010. New applications of MR sensors, such as in vehicle detection, location, and classification, are arising since 2010 [65]–[72]. As the investment on MR sensors continues to increase, their cost will be further reduced. With the proved better performance over shunt resistor and Hall-effect sensors as shown in this paper, the MR sensors are expected to become popular in current sensing of UAVs in the near future. This can boost the industry development of UAVs at large.

V. Conclusion

The results of this paper indicate that the MR sensors are the most suitable current sensors for UAVs. By adopting the relative scoring method, it is observed that the MR sensors perform better than the Hall-effect sensors and the fluxgate sensors. Through the comparison by a radar graph, the MR sensors have higher accuracy, consume less energy, endure wider temperature variation, and more compact than the Hall-effect current sensors, which benefits them to be integrated into UAVs. The MR sensors are also very competitive with traditional shunt resistors through the overall comparison. This finding provides insight into the selection strategy of current sensors for UAVs and can enhance the industrial development of UAV potentially.

References

[1] K. Zhu and P. W. T. Pong, "Performance study on commercial magnetic sensors for measuring current of unmanned aerial vehicles," in *Proc. IEEE Int. Instrum. Meas. Technol. Conf.*, May 2018, pp. 2178–2180.

[2] Markets. (2018). *Unmanned Aerial Vehicle (UAV) Market by Application*. Accessed: Mar. 30, 2018. [Online]. Available: https://www.marketsandmarkets.com/Market-Reports/unmanned-aerial-vehicles-uav-market-662.html

[3] P. Van Blyenburgh, "UAVs: An overview," *Air Space Eur.*, vol. 1, pp. 43–47, Sep./Dec. 1999.

[4] D. W. Casbeer, R. W. Beard, T. W. McLain, S.-M. Li, and R. K. Mehra, "Forest fire monitoring with multiple small UAVs," in *Proc. IEEE Conf. Amer. Control*, Jun. 2005, pp. 3530–3535.

[5] D. Kingston, R. W. Beard, and R. S. Holt, "Decentralized perimeter surveillance using a team of UAVs," *IEEE Trans. Robot.*, vol. 24, no. 6, pp. 1394–1404, Dec. 2008.

[6] M. Rossi and D. Brunelli, "Autonomous gas detection and mapping with unmanned aerial vehicles," *IEEE Trans. Instrum. Meas.*, vol. 65, no. 4, pp. 765–775, Apr. 2016.

[7] K. Zhu and P. W. T. Pong, "Curved trapezoidal magnetic flux concentrator design for current measurement of multi-core power cable with magnetic sensing," *IEEE Trans. Magn.*, vol. 55, no. 4, Apr. 2019, Art. no. 4001809.

[8] Chris Winkler. (2016). *How Many Sensors are in a Drone, And What do they Do?* Accessed: Jul. 3, 2018. [Online]. Available: https://www.sensorsmag.com/components/how-many-sensors-are-a-drone-and-what-do-they-do

[9] OscarLiang. (2013). *Monitor Battery of UAVs*. Accessed: Mar. 27, 2018. [Online]. Available: https://buff.ly/2Gahis9

[10] P. Daponte, L. De Vito, F. Lamonaca, F. Picariello, S. Rapuano, and M. Riccio, "Measurement science and education in the drone times," in *Proc. IEEE Conf. Instrum. Meas. Technol.*, May 2017, pp. 1–6.

[11] X. Xua and A. Anvar, "Intelligent condition monitoring system (ICMS) for unmanned air vehicle (UAV), unmanned surface vehicle (USV) and autonomous underwater vehicle (AUV), robots: A feasibility study," in *Proc. Int. Congr. Modelling Simulation*, 2013, pp. 1–7.

[12] Texas Instruments. (2015). *BQ2013H*. Accessed: Jul. 3, 2018. [Online]. Available: http://www.ti.com/lit/ds/slus120b/slus120b.pdf

[13] M. Podhradský, J. Bone, C. Coopmans, and A. Jensen, "Battery model-based thrust controller for a small, low cost multirotor unmanned aerial vehicles," in *Proc. Int. Conf. Unmanned Aircr. Syst.*, 2013, pp. 105–113.

[14] E. Mueller, "Hardware-in-the-loop simulation design for evaluation of unmanned aerial vehicle control systems," in *Proc. Conf. Exhibit Modeling Simulation Technol.*, 2007, pp. 1–14.

[15] D. Jung *et al.*, "Design and development of a low-cost test-bed for undergraduate education in UAVs," in *Proc. IEEE Conf. Decis. Control*, Dec. 2005, pp. 2739–2744.

[16] A. Sanchez, L. R. G. Carrillo, E. Rondon, R. Lozano, and O. Garcia, "Hovering flight improvement of a quad-rotor mini UAV using brushless DC motors," *J. Intell. Robot. Syst.*, vol. 61, pp. 85–101, Jan. 2011.

[17] M. P. MacMartin and N. L. Kusters, "A direct-current-comparator ratio bridge for four-terminal resistance measurements," *IEEE Trans. Instrum. Meas.*, vol. 15, no. 4, pp. 212–220, Dec. 1966.

[18] Multi Dimension. (2015). *Introduction to TMR Magnetic Sensors*. Accessed: Jul. 3, 2018. [Online]. Available: http://www.dowaytech.com/en/1776.html

[19] J. E. Lenz, "A review of magnetic sensors," *Proc. IEEE*, vol. 78, no. 6, pp. 973–989, Jun. 1990.

[20] W. Li, C. Mao, and J. Lu, "Study of the virtual instrumentation applied to measure pulsed heavy currents," *IEEE Trans. Instrum. Meas.*, vol. 54, no. 1, pp. 284–288, Feb. 2005.

[21] T. M. R. Baião, "Energy monitoring system for low-cost UAVs," M.S. thesis, Mech. Eng. Inst., Instituto Superior Técnico, Lisboa, Portugal, 2017.

[22] Y. Jin, A. A. Minai, and M. M. Polycarpou, "Cooperative real-time search and task allocation in UAV teams," in *Proc. IEEE Conf. Decis. Control*, Dec. 2003, pp. 7–12.

[23] Unmanned Systems Technology. (2017). *Battery Management Systems*. Accessed: 10-Jul. 10, 2018. [Online]. Available: http://www.unmannedsystemstechnology.com/category/supplier-directory/propulsion-power/battery-management-systems-bms-battery-packs/

[24] B. Saha *et al.*, "Battery health management system for electric UAVs," in *Proc. Conf. Aerosp.*, 2011, pp. 1–9.

[25] A. Malaver, N. Motta, P. Corke, and F. Gonzalez, "Development and integration of a solar powered unmanned aerial vehicle and a wireless sensor network to monitor greenhouse gases," *Sensors*, vol. 15, no. 2, pp. 4072–4096, 2015.

[26] Bill Gabbert. (2011.)*At What Temperature Does a Forest Fire Burn?* Accessed: Jul. 12, 2016. [Online]. Available: http://wildfiretoday.com/2011/02/26/at-what-temperature-does-a-forest-fire-burn/

[27] B. Loth, H.-F. Graf, and J. M. Oberhuber, "Snow cover model for global climate simulations," *J. Geophys. Res., Atmos.*, vol. 98, pp. 10451–10464, Jun. 1993.

[28] J.-H. Kim, S. Sukkarieh, and S. Wishart, "Real-time navigation, guidance, and control of a UAV using low-cost sensors," in *Field and Service Robotics*, vol. 24. Cham, Switzerland: Springer, 2003, pp. 299–309.

[29] Rob Wile. (2017). *Why High-End Drones Are Half the Price They Were a Year Ago*. Accessed: Jul. 22, 2018. [Online]. Available: http://time.com/money/4800984/drone-prices-decrease-spark-dji/

[30] Rise Global. (2018). *Relative Scoring vs. Absolute Scoring*. Accessed: Jul. 10, 2018. [Online]. Available: http://help.leaderboarded.com/knowledgebase/articles/613299-relative-scoring-vs-absolute-scoring-explained.

[31] HELIPAL. (2018). *DJI F450 GPS Drone*. Accessed: Jul. 4, 2018. [Online]. Available: http://www.helipal.com/dji-f450-w-naza-v2-and-h3-2d-gimbal-rtf.html

[32] WIRED. (2017). *How do Drones Fly?* Accessed: Jul. 7, 2018. [Online]. Available: https://www.wired.com/2017/05/the-physics-of-drones/

[33] Allegro. (2018). *ACS712 Questions*. Accessed: Mar. 31, 2018. [Online]. Available: https://buff.ly/2pU22p6

[34] Speake & Co Llanfapley. (2010). *FGM-3*. Accessed: Mar. 30, 2018. [Online]. Available: https://buff.ly/2J8M7LQ

[35] Sensorland. (2018). *What is a Fluxgate?* Accessed: Jul. 5, 2018. [Online]. Available: http://www.sensorland.com/HowPage071.html

[36] Honeywell. (2010). *1, 2 and 3 Axis Magnetic Sensors HMC1051/HMC1052L/HMC1053*. Accessed: Oct. 3, 2018. [Online]. Available: https://aerocontent.honeywell.com/aero/common/documents/myaerospacecatalog-documents/Defense_Brochures-documents/HMC_1051-1052-1053_Data_Sheet.pdf

[37] Honeywell. (2018). *Three-Axis Magnetic Sensor HMC1043L*. Accessed: Oct. 3, 2018. [Online]. Available: https://aerocontent.honeywell.com/aero/portal/Common/Documents/myaerospacecatalog-documents/Space_brochures-documents/HMC1043L_3-Axis_Magnetic_Sensor_PRELIMINARY.pdf

[38] Multi Dimension. (2018). *TMR2301*. Accessed: Oct. 3, 2018. [Online]. Available: https://www.aecsensors.com/components/com_virtuemart/shop_image/product/Magnetic-Tunnelling-Magnetoresistive-(TMR)-Linear-Sensors/pdfs/TMR2301-datasheet.pdf

[39] Multi Dimension. (2018). *TMR9002*. Accessed: Oct. 3, 2018. [Online]. Available: https://www.aecsensors.com/components/com_virtuemart/shop_image/product/Magnetic-Tunnelling-Magnetoresistive-(TMR)-Linear-Sensors/pdfs/TMR9002-datasheet.pdf

[40] NVE. *AA/AB-Series Analog Magnetic Sensors*. Accessed: Oct. 3, 2018. [Online]. Available: https://www.nve.com/Downloads/analog_catalog.pdf

[41] SENSITEC. (2015). *GF708*. Accessed: Oct. 3, 2018. [Online]. Available: https://www.sensitec.com/fileadmin/sensitec/Service_and_Support/Downloads/Data_Sheets/GF700/SENSITEC_GF708_DSE_05.pdf

[42] ARCOL. (2018). *CRS Shunt Resistor*. Accessed: Oct. 3, 2018. [Online]. Available: https://www.mouser.hk/datasheet/2/303/CRS-1-14.23-1297859.pdf

[43] M. Nowicki, M. Kachniarz, and R. Szewczyk, "Temperature error of Hall-effect and magnetoresistive commercial magnetometers," *Arch. Elect. Eng.*, vol. 66, no. 3, pp. 625–630, 2017.

[44] Zettlex. (2018). *Magnetic Position Sensors*. Accessed: Mar. 30. 2018. [Online]. Available: https://buff.ly/2pRh6TO

[45] J. Schappert and F. H. Wians, "A novel use of radar graphs in evaluating the operational performance characteristics of laboratory instruments," *Lab. Med.*, vol. 37, no. 11, pp. 679–683, 2006.

[46] C. Duret and S. Ueno, "TMR: A new frontier for magnetic sensing," *NTN Tech. Rev.*, vol. 80, pp. 64–71, Oct. 2012.

[47] Honeywell. (2003). *Magnetoresistive Sensors*. Accessed: Jul. 12, 2018. [Online]. Available: https://sensing.honeywell.com/index.php?ci_id=50272&la_id=1

[48] OTO Technology. (2017). *The Evolution of Magnetic Sensing Technology*. Accessed: Jul. 7, 2018. [Online]. Available: https://disti-assets.s3.amazonaws.com/testco-inc/files/datasheets/25049.pdf

[49] M. Looney, "Analog devices," Analog Devices, Inc., Norwood, MA, USA, Appl. Note AN07538-0-5/09(0), 2009. Accessed: Oct. 19. 2018. [Online]. Available: https://www.analog.com/media/en/technical-documentation/application-notes/AN-0970.pdf

[50] Electronics. (2018). *Hall Effect Sensors*. Accessed: Jul, 5, 2018. [Online]. Available: https://www.electronics-tutorials.ws/electromagnetism/hall-effect.html

[51] Honeywell. (2018). *Set/Reset Pulse Circuits for Magnetic Sensors*. Accessed: Oct. 18, 2018. [Online]. Available: https://neurophysics.ucsd.edu/Manuals/Honeywell/AN-201.pdf

[52] X. Liu *et al.* (2016). "Overview of spintronic sensors, Internet of Things, and smart living." [Online]. Available: https://arxiv.org/abs/1611.00317

[53] Multi Dimension. (2018). *Introduction to TMR Magnetic Sensors*. Accessed: Oct. 19, 2018. [Online]. Available: http://www.dowaytech.com/en/1776.html

[54] L. Jogschies *et al.*, "Recent developments of magnetoresistive sensors for industrial applications," *Sensors*, vol. 15, no. 11, pp. 28665–28689, 2015.

[55] P. Ripka, M. Janosek, and M. Butta, "Crossfield sensitivity in AMR sensors," *IEEE Trans. Magn.*, vol. 45, no. 10, pp. 4514–4517, Oct. 2009.

[56] P. Ripka, M. Janosek, M. Butta, S. W. Billingsley, and E. Wakefield, "Crossfield effect in magnetic sensors," in *Proc. Conf. Sensors*, 2009, pp. 1860–1863.

[57] K. Zhu and P. W. T. Pong, "Curved trapezoidal magnetic flux concentrator design for improving sensitivity of magnetic sensor in multi-conductor current measurement," in *Proc. Int. Symp. Next-Gener. Electron. (ISNE)*, 2016, pp. 1–2.

[58] R. P. Oberlin and J. P. Blatt, "Lithium battery system," U.S. Patent 20080084182 A1, Apr. 10, 2008.

[59] X. Xua and A. Anvara, "Intelligent condition monitoring system (ICMS) for unmanned air vehicle (UAV), unmanned surface vehicle (USV) and autonomous underwater vehicle (AUV), robots: A feasibility study," in *Proc. Int. Congr. Modelling Simulation*, 2013, pp. 1–7.

[60] J. Lenz and A. S. Edelstein, "Magnetic sensors and their applications," *IEEE Sensors J.*, vol. 6, no. 3, pp. 631–649, Jun. 2006.

[61] M. Jullière, "Tunneling between ferromagnetic films," *Phys. Lett. A*, vol. 54, no. 3, pp. 225–226, Sep. 1975.

[62] M. N. Baibich *et al.*, "Giant magnetoresistance of (001)Fe/(001)Cr magnetic superlattices," *Phys. Rev. Lett.*, vol. 61, p. 2472, Nov. 1988.

[63] B. Dieny, V. S. Speriosu, S. S. P. Parkin, B. A. Gurney, D. R. Wilhoit, and D. Mauri, "Giant magnetoresistive in soft ferromagnetic multilayers," *Phys. Rev. B, Condens. Matter*, vol. 43, no. 1, p. 1297, Jan. 1991.

[64] T. Miyazaki and N. Tezuka, "Giant magnetic tunneling effect in Fe/Al_2O_3/Fe junction," *J. Magn. Magn. Mater.*, vol. 139, pp. L231–L234, Jan. 1995.

[65] M. J. Caruso, "Applications of magnetoresistive sensors in navigation systems," Honeywell Inc., Charlotte, NC, USA, SAE Tech. Paper 0148-7191, 1997.

[66] J. Včelák, P. Ripka, J. Kubík, A. Platil, and P. Kašpar, "AMR navigation systems and methods of their calibration," *Sens. Actuators A, Phys.*, vol. 123, pp. 122–128, Sep. 2005.

[67] M. A. Cordoba, "Attitude and heading refernce system I-AHRS for the EFIGENIA autonomous unmanned aerial vehicles UAV based on MEMS sensor and a neural network strategy for attitude estimation," in *Proc. Medit. Conf. Control Automat.*, 2007, pp. 1–8.

[68] H. S. Guo, B. Yan, and Z. D. Wu, "Attitude measurement system with low power consumption for underwater observation platform," *Torpedo Technol.*, vol. 3, p. 7, 2013.

[69] J. Pelegri, J. Alberola, and V. Llario, "Vehicle detection and car speed monitoring system using GMR magnetic sensors," in *Proc. 28th Annu. Conf. Ind. Electron. Soc.*, 2002, pp. 1693–1695.

[70] Y.-C. Lai, S.-S. Jan, and F.-B. Hsiao, "Development of a low-cost attitude and heading reference system using a three-axis rotating platform," *Sensors*, vol. 10, no. 4, pp. 2472–2491, Mar. 2010.

[71] X. Zhou, "Vehicle location estimation based on a magnetic sensor array," in *Proc. IEEE Sensors Appl. Symp.*, 2013, pp. 80–83.

[72] B. Yang and Y. Lei, "Vehicle detection and classification for low-speed congested traffic with anisotropic magnetoresistive sensor," *IEEE Sensors J.*, vol. 15, no. 2, pp. 1132–1138, Feb. 2015.

Ke Zhu was born in Yichang, China, in 1990. He received the B.Eng. degree in electrical engineering from China Three Gorges University (CTGU), Yichang, in 2013, and the Ph.D. degree in electrical and electronic engineering from The University of Hong Kong (HKU), Hong Kong, in 2018.

He is currently a Post-Doctoral Researcher with The University of Hong Kong. His current research interests include computational electromagnetics, electric power transmission monitoring, and application of magnetoresistive (MR) sensors in smart grid.

Xuyang Liu (S'16) received the B.Eng. degree from the University of Electronic Science and Technology of China (UESTC), Chengdu, China, in 2015. He is currently pursuing the Ph.D. degree with the Department of Electrical and Electronic Engineering, The University of Hong Kong, Hong Kong.

His current research interests include nondestructive testing, advanced sensing technologies, and applications of magnetoresistive magnetic field sensors in electric vehicles and wireless power transfer.

Philip W. T. Pong (SM'12) received the B.Eng. degree (Hons.) in electrical and electronic engineering from The University of Hong Kong (HKU), Hong Kong, in 2002, and the Ph.D. degree in engineering from the University of Cambridge, Cambridge, U.K., in 2005.

He was a Post-Doctoral Researcher with the Magnetic Materials Group, National Institute of Standards and Technology (NIST), Gaithersburg, MD, USA, for three years. He joined the Department of Electrical and Electronic Engineering, HKU, in 2008, where he is currently an Associate Professor working on the development of magnetoresistive (MR) sensors and the applications of MR sensors in smart grid and smart living.

Dr. Pong is a Chartered Physicist, a Chartered Energy Engineer, a registered Professional Engineer, a fellow of the Institute of Materials, Minerals and Mining, a fellow of the NANOSMAT Society, and a Corporate Member of the Hong Kong Institution of Engineers (HKIE) in Electrical Division, Electronics Division, and Energy Division. He was a recipient of the HKIE Young Engineer of the Year Award in 2016. He is serving on the Administrative Committee of the IEEE Magnetics Society. He serves as an Editorial Board Member for three SCI journals.